NUCL SCI TECH (2017) 28:75
DOI 10.1007/s41365-017-0232-9

Alignment of beam position monitors in cryomodule of CADS injector II

Jian-Dong Yuan[1] · Yuan He[1] · Bin Zhang[1] · Jun-Hui Zhang[1] · Jun-Xia Wu[1] · Yong Zhang[1] · Feng-Feng Wang[1] · Jun-Jie Yao[1] · Guo-Zhen Sun[1] · Yu-Qin Wan[1]

Received: 7 June 2016 / Revised: 10 January 2017 / Accepted: 19 January 2017 / Published online: 28 April 2017

Abstract Significant temperature difference (300–77 K or even 4 K) can cause large deformations and displacements of the beam position monitors (BPMs), which affect BPMs measurement resolution or even cause their malfunction in cryogenic situations. In this paper, to check the offset from the mechanical to electrical center in low temperature (77 K), Fourier's law and finite element method are used to simulate cryo-deformation. Laser tracker and micro-alignment telescope are employed in combined BPM calibration, installation and monitoring. The calibration error is <0.02 mm, and the installation and monitoring precision are 0.06 mm and 0.01 mm, respectively. The monitored cryo-deformation agrees well with the simulation results. These indicate that the combined alignment can improve performance of the BPM system. All these guaranteed the success of running the 9.55 MeV@2.14 mA cw protons.

Keywords Beam position monitors · Alignment · Fourier's Law · Cryomodule · CADS · ANSYS

1 Introduction

Beam position monitors (BPMs) monitor the phase and transverse position of the beam [1] in an accelerator by obtaining the difference ratio over the sum voltage between two opposite pick-ups. Button BPMs are essential and the only diagnostics components in cryomodule of injector II in the Chinese Accelerator Driven Sub-critical system (CADS) [2], and their alignment must be considered carefully. Due to manufacturing uncertainties in radius, location and symmetry of the electrodes, BPMs measurements deviate from the nominal values [3, 4]. To improve the measurement accuracy, button BPMs have to be calibrated before installation [5]. There were excellent studies concentrated on the calibration using an antenna [4, 6, 7] or a stretched wire method [2, 8, 9] at room temperature. However, few reports are available on installation of the BPMs to work at 77 or 4 K, as deformation shall be caused by different temperatures [10]. Lipka et al. [11] studied electrical and mechanical properties of button BPMs in cryogenic environments, and addressed the necessity of assembling and installing BPMs in a clean room. Zhu et al. [12] reported the wire position monitor method of a cryomodule at IHEP, without comparing the aligned results with beam-based alignment (BBA), though.

To guarantee the required uncertainty of alignment (calibration ≤0.02 mm, displacement of installation ≤0.06 mm, rotation of installation ≤3 mrad, monitoring precision in 77 K ≤ 0.1 mm), we propose, in this paper, a method of using a micro-alignment telescope plus a laser tracker and compared the results with BBA. The paper is organized as follows In Sect. 2, mechanic structure of the BPMs is briefly described, and details are given on the entire aligned process using a laser tracker plus a micro-alignment telescope. In Sect. 3, simulation results using finite element methods are compared with the monitoring results. In Sect. 4, we present the calibration results adopting portable coordinate measurement machine and the BBA, and discuss the aligned accuracy, which fulfills

This work was supported by the National Natural Science Foundation of China (No. 11605262).

✉ Jian-Dong Yuan
yuanjiandong@impcas.ac.cn

[1] Institute of Modern Physics, Chinese Academy of Sciences, Lanzhou 730000, China

the requirements and guarantees the success of running the 9.55 meV@ 2.14 mA cw protons. Research on cold alignment of the BPM system is of help for its fabrication and application.

2 Mechanic structure and alignment

2.1 Mechanic structure

As shown in Fig. 1, BPMs are fixed on rear of the solenoid. The 3D translation stage moves, driven by step motors, along the *X*-, *Y*- and *Z*-axes with a precision of 1 μm in the closed-loop control. A BPM is small enough to be installed in a restricted space of the cryomodule. The vacuum aperture is 40 mm and the longitudinal length is 180 mm. The gap between the beam pipe and button along the longitudinal direction is 3.4 mm. We use four coupling electrodes to measure the horizontal and vertical position of the beam [11]. According to the equivalent capacity coupling model [6], Eq. (1) is used to calculate the normalized horizontal *X* and vertical *Y* positions with the mechanical center, where K_X and K_Y are the geometric coefficients of BPM and are the reciprocal of sensitivity (in mm); $V_{\text{A–D}}$ are the voltages on the corresponding electrodes scaled with the appropriate calibration coefficients; and X_{offset} and Y_{offset} are the offset between mechanic and electronic center.

$$\begin{aligned} X &= K_X \frac{V_\text{A} - V_\text{C}}{V_\text{A} + V_\text{C}} + X_\text{offset} \\ Y &= K_Y \frac{V_\text{B} - V_\text{D}}{V_\text{B} + V_\text{D}} + Y_\text{offset} \end{aligned} \tag{1}$$

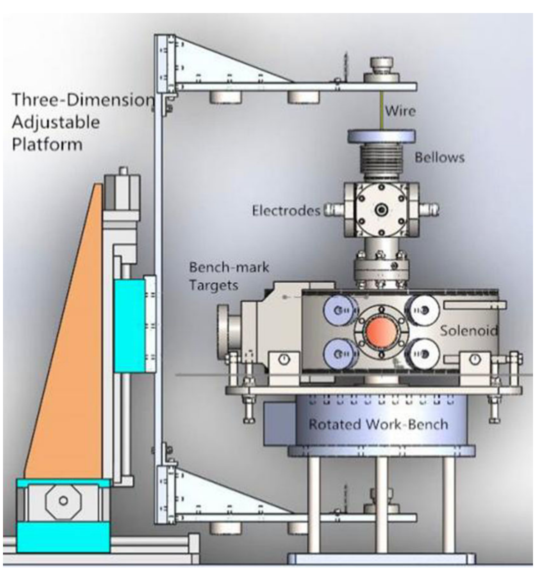

Fig. 1 Rotating workbench

The BPM measurement covers trajectory, first turn, equilibrium, turn-by-turn, beam-based alignment and orbit stability [13, 14]. To meet requirements of the superconductor cavity, button BPMs in cryomodule are expected to operate under ultra-high vacuum conditions, cryogenic environments and a clean room class 100 certification. Hence, a precise alignment is required for the BPMs not only in the initial installation, but also a regular control of their actual position and the preservation of their nominal values over a long period. These are essential for an undisturbed operation of a machine or an experiment. The alignment procedure includes calibration, installation and monitoring.

2.2 Calibration

The calibration is to determinate the center of BPMs, reduce the coordinate error as much as possible and transfer the data to external targets settled on the solenoid [15]. Figure 2 shows the calibration bench, on which both mechanical and electrical methods are used. The mechanic method contains initial calibration of the individual solenoid, assembly, and calibration of the combined BPMs and solenoids. The initial calibration is performed by a portable coordinate measurement machine (CMM) with eight benchmark targets. The frame's origin is the mechanic center of the combined BPM and solenoid. The *Y*-axis is purely vertical with opposite sign. The *Z*-axis is along the beam direction, and the *X*-axis is perpendicular to both the *Y*- and *Z*-axes. The signs are determined by the right-hand rule. Assembly the BPM in a clean room has an influence on the friction forces of bolts and nuts and the

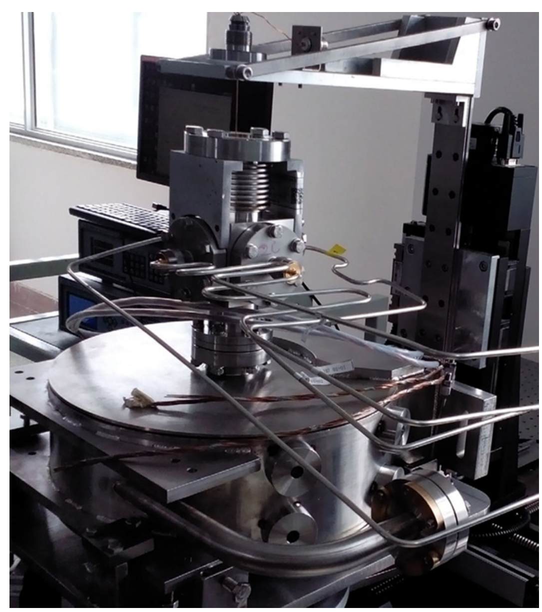

Fig. 2 Calibration bench setup

methodical steps of the assembly [11]. Therefore, to optimize the assembly and avoid deformation of the flanges from the excessive strength, according to simulation results, the torque is restricted to 5 N m. The mechanic offsets for the assembly and alignment of BPMs are obtained on the designed workbench, as the error of fiducial target is not avoidable from the manufacturer [16].

The electrical calibration is to correlate the mechanic and electrical centers. It needs high performance of rotation symmetry, and the mechanic center should be aligned in advance to the center of rotating platform [17]. Therefore, the offset between mechanical and rotating center shall be tracked in the electrical calibration. Figure 3 shows the calibration results of mapping functions using the difference over sum at the fundamental frequency of 162.5 MHz with a Libera Single Pass H, in a square region of ±4 mm lengths in 0.2 mm steps. The four output voltages picked up from the monitor are measured at 1681 wire positions in the horizontal and vertical directions like a lattice around the BPMs center. At each wire position, the pickup voltages are measured 50 times and the average value and the errors are stored together with the wire positions on a hard disk. In the central region of ±1 mm, the distortion was less than 10 µm, while it was 20 µm at the point of ±2 mm away from the center (the inside square in Fig. 3). This distortion is acceptable for our practical application.

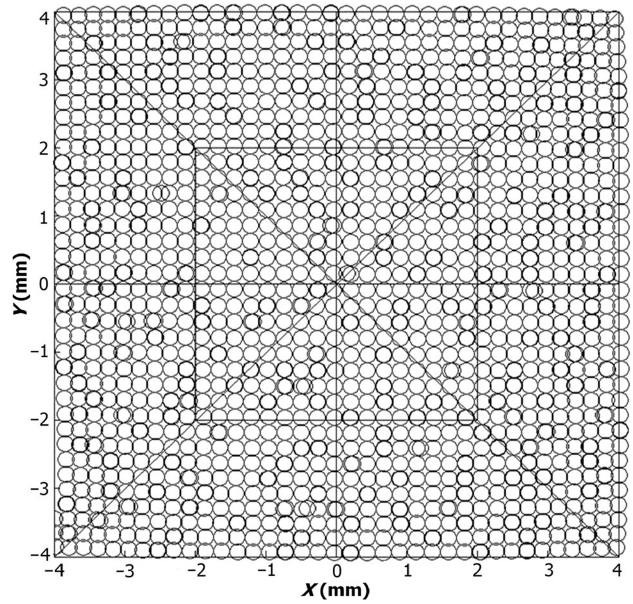

Fig. 3 Mapping

2.3 Combined installation

The combined installation used a 3D coordinate transformation to uniform spatial frame. There are three models: Bursa, Molodensky and Wu Ce. The purpose of coordinate transformation is to fulfill the start frame to the target frame with seven parameters. To restrict the displacement, rotation and scale errors within mm, $10^{-3''}$ and 10^{-7}, respectively [18], the 3D nonlinear model in Eq. (2) is used [19], independent equal precision observation, MTLS is used for transformation with any scale factor [20], without the need of iterative calculation. In the MTLS solution, both the start and target data contain random errors; therefore, the six DOF code (six degrees of freedom) is developed (Fig. 4) to limit calculation uncertainty and improve aligning accuracy. Two laser trackers in separate bilateral directions are used to improve the accuracy, avoid repeated stationing and reduce the installation time.

$$\begin{bmatrix} X \\ Y \\ Z \end{bmatrix}^i_{\text{Target}} = \begin{bmatrix} \Delta x \\ \Delta y \\ \Delta z \end{bmatrix} + (1+m)\cdot \begin{bmatrix} \cos\phi\cos\kappa & \cos\omega\sin\kappa + \sin\omega\sin\phi\cos\kappa & \sin\omega\sin\kappa - \cos\omega\sin\phi\cos\kappa \\ -\cos\phi\sin\kappa & \cos\omega\cos\kappa - \sin\omega\sin\phi\sin\kappa & \sin\omega\cos\kappa + \cos\omega\sin\phi\sin\kappa \\ \sin\phi & -\sin\omega\cos\phi & \cos\omega\cos\phi \end{bmatrix} \cdot \begin{bmatrix} X \\ Y \\ Z \end{bmatrix}^i_{\text{Origin}}, \tag{2}$$

where m is the scale factor; ω, φ and κ are rotation parameters; $\triangle x$, $\triangle y$ and $\triangle z$ are displacement factors; and i is the point number (from 1 to n).

The BPMs are sealed in the cryomodule operated at 4 K, and the structure is complex, so multivariate total least squares (MTLS) is used to realize combined installment. To coordinate with a bigger rotation angle or under

2.4 Monitoring

A micro-alignment telescope (MAT) was adopted to monitor vacuum and cooling down (77 K) displacements. Specific crosshairs was designed [21], and fiberglass (G11) was chosen as the material of cryo-crosshairs to verify the reproducibility of the horizontal and vertical position of the cold mass. As the aiming error of an optical instrument is proportional to the distance, we shortened the aiming distance and did multiple measurements to use the average [22]. To reduce the refractive error of glass, the incident angle was minimized [23]. It means that the aligning axis

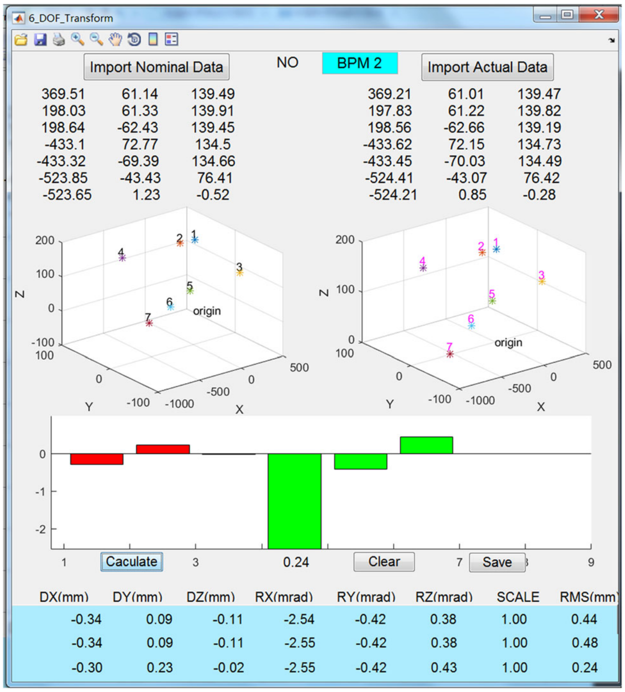

Fig. 4 (Color online) Solution of six DOF

was parallel or coincident with the normal axis of the glass. Therefore, an electronic level was used for leveling MAT within 0.05 mm/m. To avoid diffractive error of light, crosshairs were arranged at different eccentricities (±0.2 mm). To facilitate the observation, crosshairs were rotated to different angles (±30°/60°). Prior to the monitoring, the laser tracker was used to adjust the two reference targets of the telescope to a straight line, and then, the MAT was aligned to the reference line using the "Far Rotation Near Translation" method [21]. Finally, the crosshairs of each BPM were aligned to the reference target line. In the monitoring process, as the deformation and displacement were beyond the telescope range (±1.2 mm), a dial indicator (Fig. 5) was used to reduce the uncertainty error to ±0.01 mm.

3 Results and discussion

3.1 Results of simulating and monitoring

Usually, heat transfer includes the processes of thermal radiation, convection, and sometimes mass transfer. Being operated in cryo-vacuum environment, the BPMs themselves do not have convective heat transfer [24] except thermal radiation from the room environment, and thermal conduction through the cold mass supports and the feedthroughs. The finite element code of ANSYS was used to analyze the thermal stress and displacement, with Solid

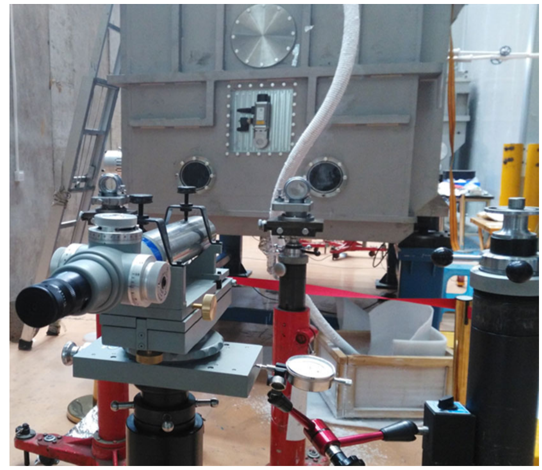

Fig. 5 Monitoring illustration used MAT

Works to construct model, meshing with four surfaces units. The cooling experiments were done with liquid nitrogen. The contact surface of support ball hinge was operated at 300 K. The surface heat load at 77 K (BPMs) was 0.9 W/m^2. The BPMs were made of stainless steel (AISI 316LN) with a weight of 5.2 kg. The loads included a self-gravity, a distributive load of temperature and the top suspending support. Temperature gradient in vertical direction is four times as much as in the horizontal direction, so the simulated horizontal and vertical cryo-displacements were 0.7 and 2.9 mm, respectively (Fig. 6a, b).

Experiments were performed with five BPMs to monitor their cryo-deformations in horizontal and vertical directions. Figure 6c shows the results in a thermal cycling. As the target was located on the right (below) of solenoid, a plus sign means that it is close to center (rise up), and a minus sign means that it is off center (go down). After 24 h vacuum pumping, the BPMs were cooled down to 77 K, and in average, they contracted 0.7 mm horizontally and 2.8 mm vertically. When the BPMs were warmed up to 290 K the vacuum is broken in 24 h, they expand in average by 0.5 mm horizontally and 1.4 mm vertically. The results indicate that the reproducibility is 0.2 mm horizontally and 1.4 mm vertically.

3.2 Results of calibration and BBA

Figure 7a shows the calibration results (five BPMs) using the "stretched wire" method, in which the BPM resolution was established by measuring the residual [25]. Electrical and mechanical reproducibility contribute to the residual offset [26]. Residual offset, i.e., the accuracy, is 0.02 mm (DX) and 0.01 mm (DY). Figure 7b shows results of the five BPMs after combined installment, three displacement factors are <0.06 mm, and three rotated factors are <3 m rad.

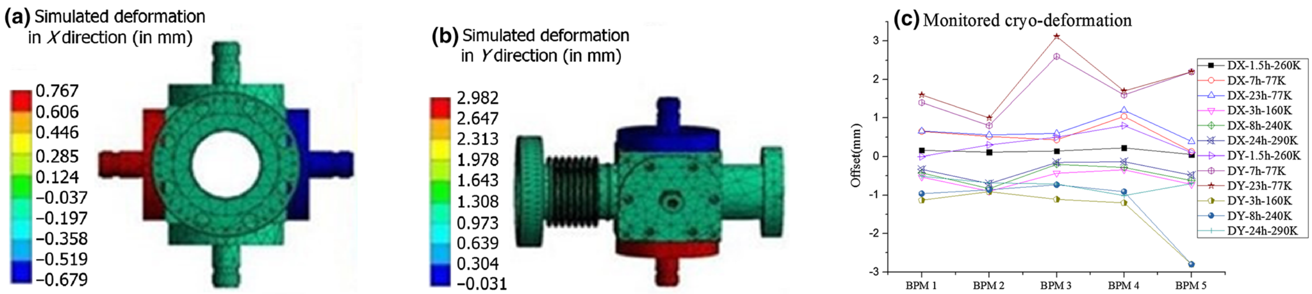

Fig. 6 (Color online) Comparison of the cryo-deformation

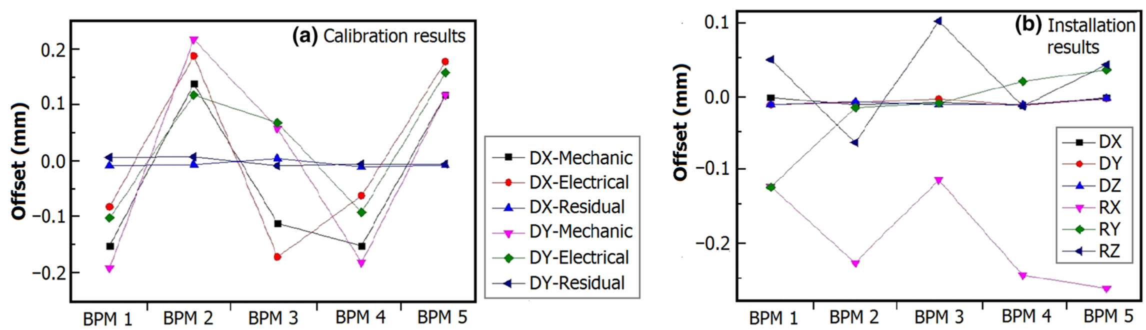

Fig. 7 (Color online) Alignment results

By correlating the magnetic center of a solenoid with a nearby BPM, we used the BBA procedure, a technique to derive the position of a quadrupole [27] or sextupole by detecting its orbit changes [28]. However, we applied the method to the solenoid by scanning the gradient of the field of solenoid one by one with a step of every 10 μA and recording all the readings of BPMs. Figure 8 shows the offset of BPM electrical center with respect to the magnetic center of the solenoid. The blue lines are the nominal simulated value, while the yellow lines are the actual measured value. As the accuracy was temperature dependent [29], and the cryo-deformation was nonlinearity from 300 to 4 K, we could not simply sum all the contributions. Also, a solenoid is incompletely equivalent to a quadrupole or a sextupole. The energy and magnetic shift are nonlinear [30]. And there was the error in alignment of the solenoid and BPMs. Even though we eliminated the two BPMs, still there was a possibility that some BPMs worked abnormally

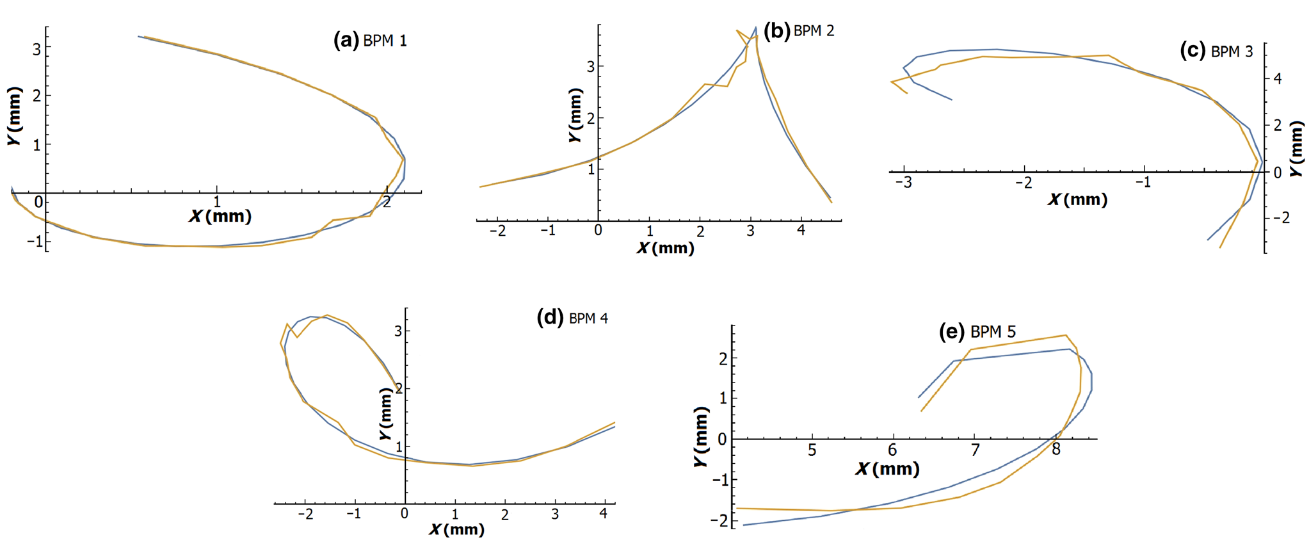

Fig. 8 (Color online) BBA results

at some specific measurements. Therefore, we obtained the offsets (0.1–0.2 mm) by comparing the measured orbit distortions with the simulated ones [27].

4 Conclusion

The BBA results indicate a rough agreement with the calibration. The alignment accuracy meets the requirements, and the combined alignment improves accuracy of BPMs. The CADS injector II began 9.55 MeV@2.14 mA proton beams recently. The running time of continuous wave with no loss of beam lasted for 20 min. We will further improve the support structure and explore the wire position monitor to realize the continuous online monitoring of BPMs.

Acknowledgements The authors thank Mrs. Young Zhang for her work in electrical calibration of BPMs and Mr. Zhi-Jun Wang for his work in the beam-based alignment.

References

1. Z.H. Li, P. Cheng, H.P. Geng et al., Physics design of an accelerator for an accelerator-driven subcritical system. Phys. Rev. Spec. Top. Accel. Beams **16**, 080101 (2013). doi:10.1103/PhysRevSTAB.16.080101
2. Y. Zhang, J.X. Wu, G.Y. Zhu et al., Capacitive beam position monitors for the low-β beam of the Chinese ADS proton linac. Chin. Phys. C **40**, 027003 (2016). doi:10.1088/1674-1137/40/2/027003
3. X.F. Hu, L. Zhao, X.S. Guo et al., A prototype of beam position and phase measurement electronics for the LINAC in ADS. Nucl. Sci. Tech. **24**, 060403 (2013). doi:10.13538/j.1001-8042/nst.2013.06.008
4. Y.L. Yang, C.C. Cheng, B.G. Sun et al., Calibration of button type beam position monitor for HIS II. Atom. Energy Sci. Technol. **48**, 541 (2014). **(in Chinese)**
5. T. Suwada, Characteristic analysis of coupled transmission lines in Stripline-type beam position monitor. Nucl. Instrum. Methods Phys. Res. A **705**, 7–12 (2013). doi:10.1016/j.nima.2012.12.069
6. J.Y. Zou, Y.L. Yang, B.G. Sun et al., Calibration of beam position monitors in the injector of HLS II, in *Proceedings of IPAC2013*, Shanghai, China, MOPME043, pp. 568–570
7. R. Johnson et al., Calibration of the beam-position monitor system for the SLAC PEP-II B factory, in *Proceeding of 1997 Particle Accelerator Conference*, Vancouver, BC, Canada (1997)
8. S. Sato, T. Tomisawa, H. Sako et al., Beam position monitor and its calibration in J-PARC linac, in *Proceedings of PAC07*, Albuquerque, New Mexico, USA, FRPMN045, pp. 4072–4074 (2007)
9. N. Hayashi, M. Kawase, S. Hatakeyama et al., Beam position monitor system of J-PARC RCS. Nucl. Instrum. Methods Phys. Res. A **677**, 94–106 (2012). doi:10.1016/j.nima.2012.02.013
10. G.B. Zhao, Y.B. Leng, R.X. Yuan et al., Analysis of thermal deformation simulation of the BPM in SSRF storage ring. Nucl. Tech. **37**, 050501 (2014). **(in Chinese)**
11. D. Lipka, B. Lorbeer, D. Nolle et al., Button BPM development for the European XFEL, in *Proceedings of DIPAC2011*, Hamburg, Germany, 2011, MOPD19, pp. 83–85
12. H.Y. Zhu, L. Dong, L.L. Men et al., Alignment of ADS beta cryostat with wire position monitor. Nucl. Sci. Tech. **26**, 040401 (2015). doi:10.13538/j.1001-8042/nst.26.040401
13. W. Daniel, Andriy A. Nosych, V. Gianluca et al., Beam feasibility study of a collimator with in-jaw beam position monitors. Nucl. Instrum. Methods Phys. Res. A **768**, 62–68 (2014). doi:10.1016/j.nima.2014.09.024
14. F.F. Wu, Z.R. Zhou, Y.L. Yang et al., Calibration method for electrode gains in an axially symmetric stripline BPM. Nucl. Sci. Tech. **25**, 050102 (2014). doi:10.13538/j.1001-8042/nst.25.050102
15. G.B. Zhao, R.X. Yuan, Z.C. Chen et al., Development of button-type pickup for SSRF ring. Nucl. Sci. Tech. **25**, 060103 (2014). doi:10.13538/j.1001-8042/nst.25.060103
16. W.H. Richard, H.H. Georg, Orbit and optics improvement by evaluating the nonlinear beam position monitor response in the Cornell Electron Storage Ring. Phys. Rev. Spec. Top. Accel. Beams **8**, 062802 (2005). doi:10.1103/PhysRevSTAB.8.062802
17. C.S. Maurice, Design, test, and calibration of an electrostatic beam position monitor. Phys. Rev. Spec. Top. Accel. Beams **13**, 032801 (2010). doi:10.1103/PhysRevSTAB.13.032801
18. W.X. Zeng, B.Z. Tao, Non-linear adjustment model of three-dimensional coordinate transformation. Geomat. Inf. Sci. Wuhan Univ. **28**(5), 566–568 (2003). **(in Chinese)**
19. D.Y. Wang, X.L. Zhang, Q. Ma et al., Procrustes method in coordinate transformation on multi-station of large-scale measurement. Opt. Precis. Eng. **22**(4), 949–955 (2014). doi:10.3788/OPE.20142204.0949. **(in Chinese)**
20. L.J. Li, Y.H. Zhao, X.Z. Lin, Application of WTLS in the coordinate transformation of laser tracker. Opt. Precis. Eng. **23**(9), 2570–2577 (2015). doi:10.3788/OPE.20152309.2570. **(in Chinese)**
21. J.D. Yuan, The alignment technology of ADS-cry module in low temperature. Chin. J. Low-Temp. Phys. **37**(2), 161–164 (2015). doi:10.13380/j.cnki.chin.j.lowtemp.phys.2015.02.015. **(in Chinese)**
22. Y.N. Jiang, Discussion on aiming error of optical instruments such as a telescope. Aeronaut. Manuf. Technol. **3**, 38–40 (1982). doi:10.16080/j.issn1671-833x.1982.03.014. **(in Chinese)**
23. F. Wang, G.Y. Li, The influence of glass refraction on angular measurement. Bull. Surv. Mapp. **10**, 32–34 (2009). **(in Chinese)**
24. R.X. Han, L. Bian, R. Ge et al., Development of vacuum barrier in 2 K transfer lines for accelerator-driven sub-critical reactor system. Chin. J. Vac. Sci. Technol. **33**(11), 1061–1064 (2013). **(in Chinese)**
25. L.G. Shen, J.H. Wang, G.C. Wang et al., Development of BPM calibrator and its application for phase II in HLS. High Power Laser Part. Beams **14**, 783 (2002). **(in Chinese)**
26. J.Y. Zou, *Development and application of injector beam position monitor system at HIS II* (University of Science and Technology of China, Hefei, 2014). **(in Chinese)**
27. Y. Li, Y.W. An, Z.P. Li et al, Beam based alignment for the transport line of CSNS, in *Proceedings of IPAC2016*, Busan, Korea, TUPMB008, pp. 1121–1123
28. Beam Based Alignment. http://www.desy.de/~sahoo/WebPage/Beam%20Based%20Alignment.htm
29. J. Beebe-Wang, Beam-based alignment in RHIC. C-A/AP/493. doi:10.2172/1109519
30. M.Z. Zhang, H.H. Li, B.C. Jiang et al., Beam based alignment of the SSRF storage ring. Chin. Phys. C **33**(4), 301–305 (2009)